J Mater Sci (2010) 45:3677–3682
DOI 10.1007/s10853-010-4413-8

Densification behavior, microstructure, and electrical properties of sol–gel-derived niobium-doped $(Bi_{0.5}Na_{0.5})_{0.94}Ba_{0.06}TiO_3$ ceramics

Hongqiang Wang · Ruzhong Zuo · Yi Liu · Jian Fu

Received: 29 October 2009 / Accepted: 11 March 2010 / Published online: 23 March 2010

Abstract Superfine powders (~100 nm) with compositions of $(1 - x)(Bi_{0.5}Na_{0.5})_{0.94}Ba_{0.06}TiO_3 + xNb^{5+}$ (BNTBT6 + xNb) with x from 0 to 0.02 were synthesized by an improved citrate sol–gel method using Nb_2O_5 as Nb^{5+} source. The sintering behavior, microstructure, and various electrical properties of BNTBT6 + xNb ceramics were investigated. The results indicated that the addition of a small amount of Nb^{5+} has no remarkable effect on the crystal structure and grain morphology, but the electrical properties of the ceramics are obviously influenced. The BNTBT6 + 0.005Nb compositions exhibit enhanced densification behavior and improved electrical properties of a piezoelectric constant $d_{33} \sim 205$ pC/N and a planar electromechanical coupling factor $k_p \sim 33\%$.

Introduction

Lead-free piezoelectric compositions of $(Bi_{0.5}Na_{0.5})_{(1-y)}Ba_yTiO_3$ ($BNTBT_{100y}$) have attracted a great deal of attention owing to the existence of a rhombohedral–tetragonal morphotropic phase boundary near $y = 0.06$–0.08, where the materials show optimum piezoelectric properties and reduced coercive field. It was reported that BNTBT6 ceramics prepared by a conventional mixed-oxide route possess relatively good piezoelectric properties of piezoelectric constant $d_{33} = 125$ pC/N, coupling factors $k_{31} = 0.19$ and $k_{33} = 0.55$ [1]. In recent years, a lot of attempts have been taken to improve their densification behavior and various electrical properties, such as through doping or different processing methods [2–12], considering the volatilization of bismuth at high sintering temperature and insufficient piezoelectric properties.

Nb_2O_5 was often used in lead zirconate titanate-based piezoelectric compositions as a soft additive, with a purpose to achieve enhanced d_{33} values and reduced coercive field [13, 14]. However, there is lack of in-depth investigation about the effect of Nb^{5+} doping on the sintering, microstructure, and electrical properties of BNTBT ceramics. Moreover, BNT-based ceramics were usually produced by a conventional mixed-oxide method [6–8], exhibiting relatively high sintering temperature (up to 1200 °C). Thus, a few efforts have recently been devoted to some wet chemical methods, for example, conventional sol–gel method [9], hydrothermal method [10, 15], mechanochemical synthesis [11], and sol–gel auto-combustion method [12, 16]. However, the densification behavior and piezoelectric properties of these compositions with relatively fine initial particle size were still insufficiently investigated. In this study, the Nb^{5+}-doped BNTBT6 compositions were prepared by an improved citrate sol–gel method using Nb_2O_5 as Nb^{5+} source, together with a detailed study on their sintering behavior and the influence of Nb^{5+} doping.

Experimental procedure

A citrate sol–gel method was used to prepare BNTBT6 + xNb ($x = 0$–0.02) powders. The raw materials used in this study are $CH_3COONa{\cdot}3H_2O$ (≥99.0%), $Bi(NO_3)_3{\cdot}5H_2O$ (≥99.0%), $Ba(CH_3COO)_2$ (≥99.0%), tetrabutyl titanate (≥98.0%), Nb_2O_5 (≥99.5%), K_2CO_3 (≥99.0%), citric acid (≥99.5%), glycol (≥99.0%), and

H. Wang · R. Zuo (✉) · Y. Liu · J. Fu
Institute of Electro Ceramics & Devices, School of Materials Science and Engineering, Hefei University of Technology, Hefei 230009, People's Republic of China
e-mail: piezolab@hfut.edu.cn

ammonia (25–28%). First, Nb_2O_5 and K_2CO_3 were mixed and calcined at 900 °C for 2 h to form a soluble potassium niobate. The chemical reactions can be written as follows:

$$Nb_2O_5 + 3K_2CO_3 = 2K_3NbO_4 + 3CO_2 \uparrow$$

$$6K_3NbO_4 + 5H_2O = 18K^+ + {Nb_6O_{19}}^{8-} + 10OH^-$$

$${Nb_6O_{19}}^{8-} + 8H^+ + 11H_2O = 6Nb(OH)_5 \downarrow$$

Then, the as-prepared potassium niobate was dissolved in distilled water and titrated by nitric acid to obtain a precipitate of niobium hydroxide. The precipitate of niobium hydroxide was washed and filtered over ten times to make sure that potassium ions were totally removed, which can be chelated with citric acid. The molar ratio of citric acid to metal cations was 1.2:1. The appropriate amount of citric acid was first dissolved into deionized water. Tetrabutyl titanate diluted in ethanol was then added slowly while a pH value of 7 was adjusted by dripping a small amount of ammonia. After being stirred at 80 °C for 1 h, a yellowish liquid was obtained. Afterward, various metal salts and glycol were introduced into the above solution, followed by a stirring process for 2 h to generate a stable transparent sol. The sol was heated at 100 °C to remove redundant solvent and to form gel. Subsequently, the gel was calcined at 600 °C for 3 h to obtain yellowish crystallite powders. The powders were pressed into discs and then sintered at 1070–1130 °C for 3 h in air. Fired-on silver paste was used as electrodes for the measurement of electrical properties. The ceramics were poled in silicone oil under a dc electric field of 4–7 kV/mm at 30–70 °C for 20 min.

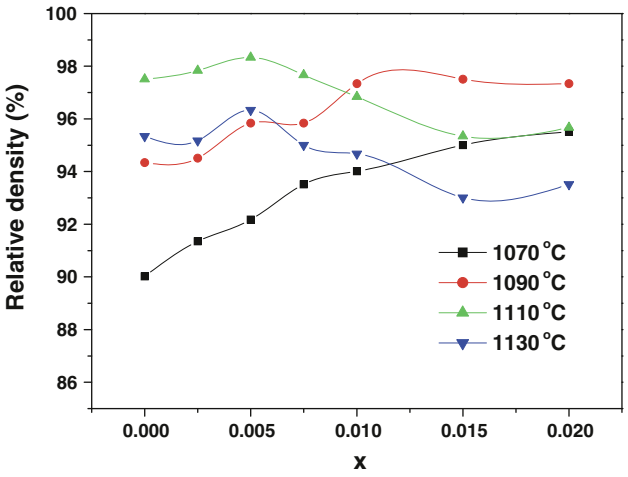

Fig. 2 Sintering behavior of BNTBT6 + *x*Nb samples as a function of Nb^{5+} content and sintering temperature as indicated

The calcined powders were characterized by a transmission electron microscope (TEM, Model H-800, Hitachi, Japan). The crystal structure of the sintered BNTBT6 + *x*Nb ceramics and the calcination condition of dry gels were determined using an X-ray diffractometer (XRD, D/Max-RB, Rigaku, Japan). The microstructure of sintered samples was observed using a scanning electron

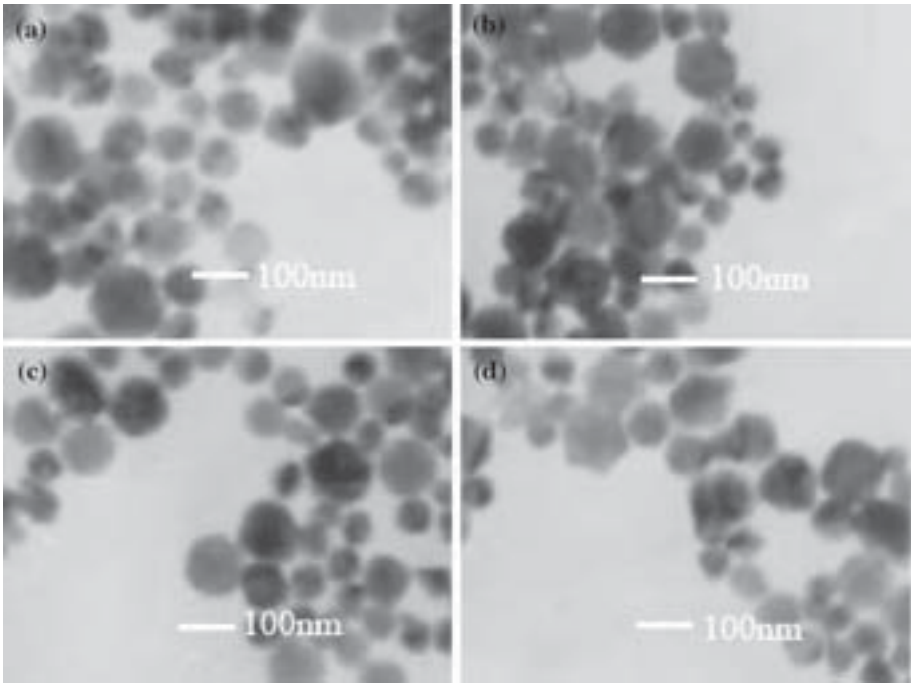

Fig. 1 TEM photographs of as-calcined BNTBT6 + *x*Nb powders prepared by a citrate method: **a** $x = 0$, **b** $x = 0.005$, **c** $x = 0.01$, and **d** $x = 0.02$

microscope (SEM, SSX-550, Shimadzu, Japan). The dielectric constant was measured as a function of temperature using a LCR meter (Agilent E4980A, USA). The piezoelectric constant d_{33} was measured directly on a quasi-static d_{33} meter (YE2730A, Sinocera, China). The electromechanical coupling coefficient k_p was measured using a high precision impedance analyzer (PV70A, Beijing Band ERA Co., Ltd. China). Polarization hysteresis loops were measured using a ferroelectric measuring system (Precision LC, Radiant Technologies, Inc. USA).

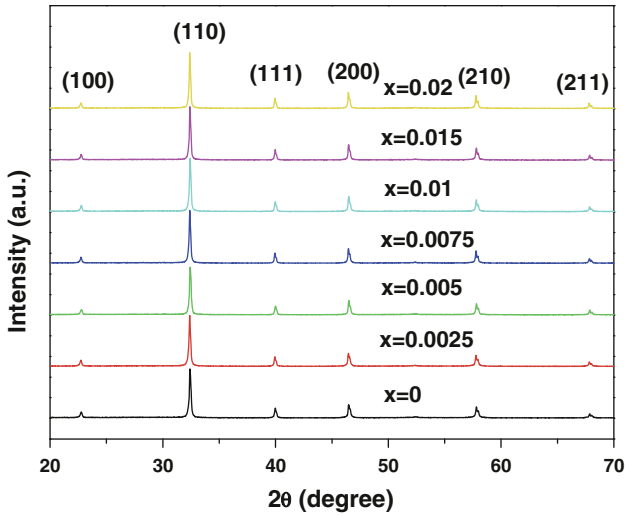

Fig. 3 XRD patterns of BNTBT6 + xNb ceramics sintered at 1110 °C

Results and discussion

Figure 1 indicates the particle morphology of as-prepared BNTBT6 + xNb powders prepared by a citrate sol–gel method. It can be seen that all crystalline particles are well dispersed with only a very slight degree of soft agglomeration. The powders with different contents of Nb^{5+} have similar morphology, and the particles are about 100 nm or less in size. It is suggested that the addition of Nb^{5+} does not cause an obvious change in the grain morphology and size after a calcination process. Moreover, the synthesizing processing proves successful, leading to the attainment of superfine powders.

Figure 2 shows the densification behavior of BNTBT6 + xNb samples as a function of Nb^{5+} content. It can be found that the sample's density exhibits a slight increase before x is less than 0.005, then a decrease afterward. The maximum density is about 5.91 g/cm^3 (~98.3% of theoretical density) for BNTBT + 0.005Nb samples sintered at 1110 °C. Furthermore, the sintering temperature generally drops slightly on increasing the amount of Nb^{5+}. It is supposed that the formation of A-site vacancies contributes to the improved sinterability based on enhanced mass transportation ability. As the content of Nb^{5+} is higher, the densification tends to be degraded slightly, probably because the melting point of Nb^{5+}-doped BNTBT6 ceramics increases with the Nb^{5+} content. The XRD patterns in Fig. 3 show that all the samples display a pure perovskite structure without detectable impurity phases, implying that Nb^{5+} ion can diffuse into the lattice of BNTBT6 within the studied doping level. No evident

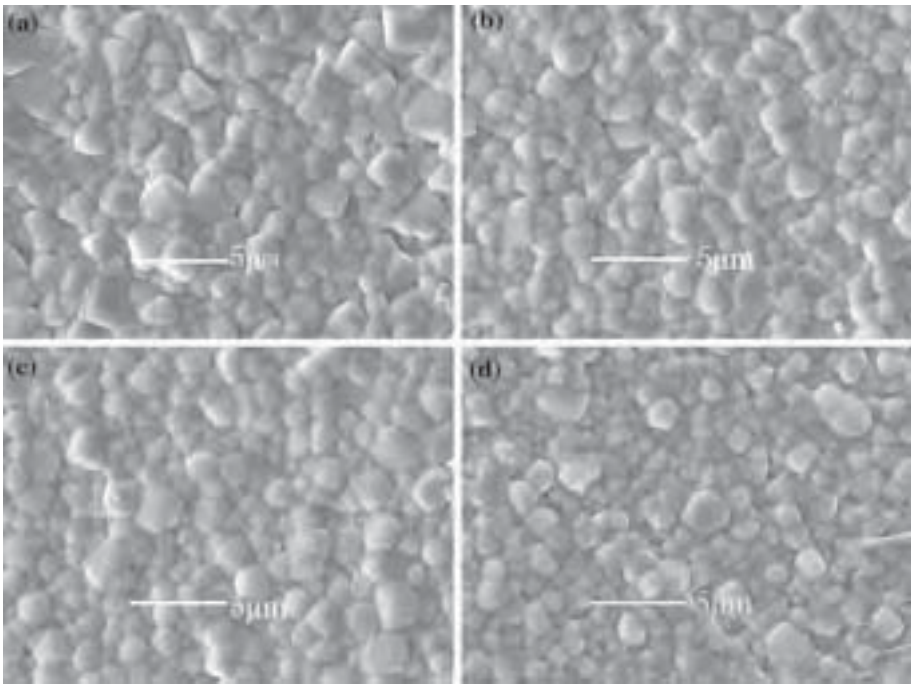

Fig. 4 SEM morphology of BNTBT6 + xNb ceramics with various Nb^{5+} contents sintered at 1110 °C for 3 h: **a** $x = 0$, **b** $x = 0.005$, **c** $x = 0.01$, and **d** $x = 0.02$

diffraction peak shift can be observed, suggesting that the lattice of BNTBT6 does not obviously change. The possible reason is that a slight expansion from the replacement of Nb^{5+} for Ti^{4+} (CN = 6, $R_{Nb}{}^{5+} = 0.64$ Å and $R_{Ti}{}^{4+} = 0.61$ Å) [17] counteracts the lattice shrinkage from the formed A-site vacancies.

The microstructure of BNTBT6 + xNb ceramics sintered at 1110 °C for 3 h is shown in Fig. 4. It is obvious that all the samples have dense microstructures and similar grain morphology with an average grain size of ~2 μm. The Archimedes method gave a relative density of more than 96% of the theoretical values for all samples, as discussed in Fig. 2. However, Nb^{5+} doping has no evident effect on the grain growth and only a very slight decrease in grain size can be seen as the Nb^{5+} content is high (for example, $x = 0.02$). This is probably associated with the pinning effect of grain boundary from A-site vacancies formed owing to the substitution of Nb^{5+} for Ti^{4+}.

As shown in Fig. 5a, the dielectric constant at 1 kHz of BNTBT6 + xNb ceramics was measured as a function of temperature. There are two dielectric anomalies at T_d and T_m, respectively. T_d refers to the transition temperature between rhombohedral ferroelectric phase (F_R) and tetragonal anti-ferroelecteric phase (AF_T), and T_m represents the temperature at which the dielectric constant reaches the maximum and corresponds to the transition from anti-ferroelecteric phase to paraelectric phase. It is clear that the dielectric maxima at T_m become significantly lower due to the addition of Nb^{5+}, meaning that Nb^{5+} acts as a suppressor, because the dielectric maxima significantly decrease with the increase of the Nb^{5+} content. Simultaneously, the anti-ferroelecteric phase zone gets broader. Moreover, the addition of Nb^{5+} decreases T_d dramatically, while T_m is only slightly reduced. These results reveal that Nb^{5+} doping tends to strengthen anti-ferroelectric states of BNTBT6 ceramics. The dielectric loss of BNTBT6 + xNb ceramics is shown in Fig. 5b. It can be seen that there are anomalies approximately at T_d, showing the same tendency with the Nb^{5+} content as for the dielectric constant.

The polarization versus electric field (P–E) hysteresis loops of BNTBT6 + xNb ceramics at various measuring temperatures are shown in Fig. 6. It can be seen that Nb^{5+} doping has a significant effect on the ferroelectric properties of BNTBT6 ceramics. At room temperature (Fig. 6a), BNTBT6 + xNb ceramics are typically ferroelectric as x is less than 0.005, while they exhibit double hysteresis loops typical for an anti-ferroelectric phase when x is above 0.005. Furthermore, the addition of a small amount of Nb^{5+} ($x < 0.005$) tends to slightly reduce the coercive field E_c, implying that Nb^{5+} act as a donor dopant. Figure 6b–f show P–E hysteresis loops of BNTBT6 + xNb ceramics at elevated temperatures. It can be found that a phase transition occurs from ferroelectric to anti-ferroelectric state on

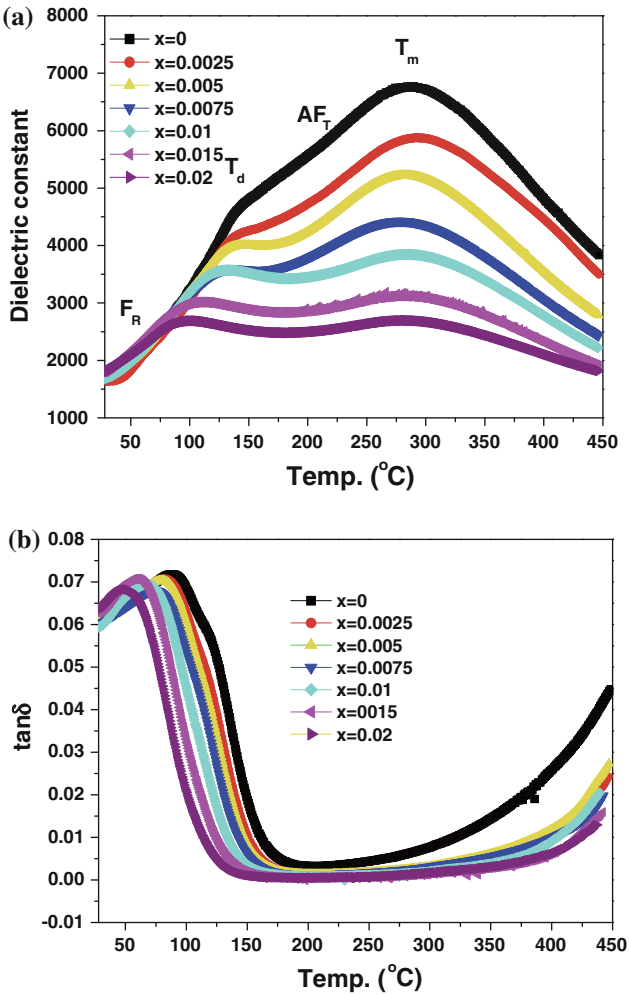

Fig. 5 Dielectric properties at 1 kHz of BNTBT6 + xNb ceramics as a function of temperature: **a** dielectric constant and **b** dielectric loss tan δ

heating, and all the samples display double hysteresis loops with increased forward switching electric fields at higher temperatures, which is associated with the reduction of T_d as discussed in Fig. 5a.

Figure 7 shows the piezoelectric and electromechanical coupling properties of BNTBT6 + xNb ceramics sintered at their individual optimum sintering temperatures (all the samples have relative densities of >97%, as seen from Fig. 2). It can be found that with the addition of Nb^{5+} less than 0.75%, both d_{33} and k_p are increased on increasing the Nb^{5+} content up to $x = 0.005$. As $x > 0.005$, these two values dramatically decrease up to nearly zero (at $x > 0.0075$), meaning that complete anti-ferroelectric states rather than ferroelectric states at room temperature appear. Enhanced piezoelectric and electromechanical coupling properties can be achieved for BNTBT6 + 0.005Nb samples. Their d_{33} and k_p can reach 205 pC/N and 33%, respectively, which almost match with the best values

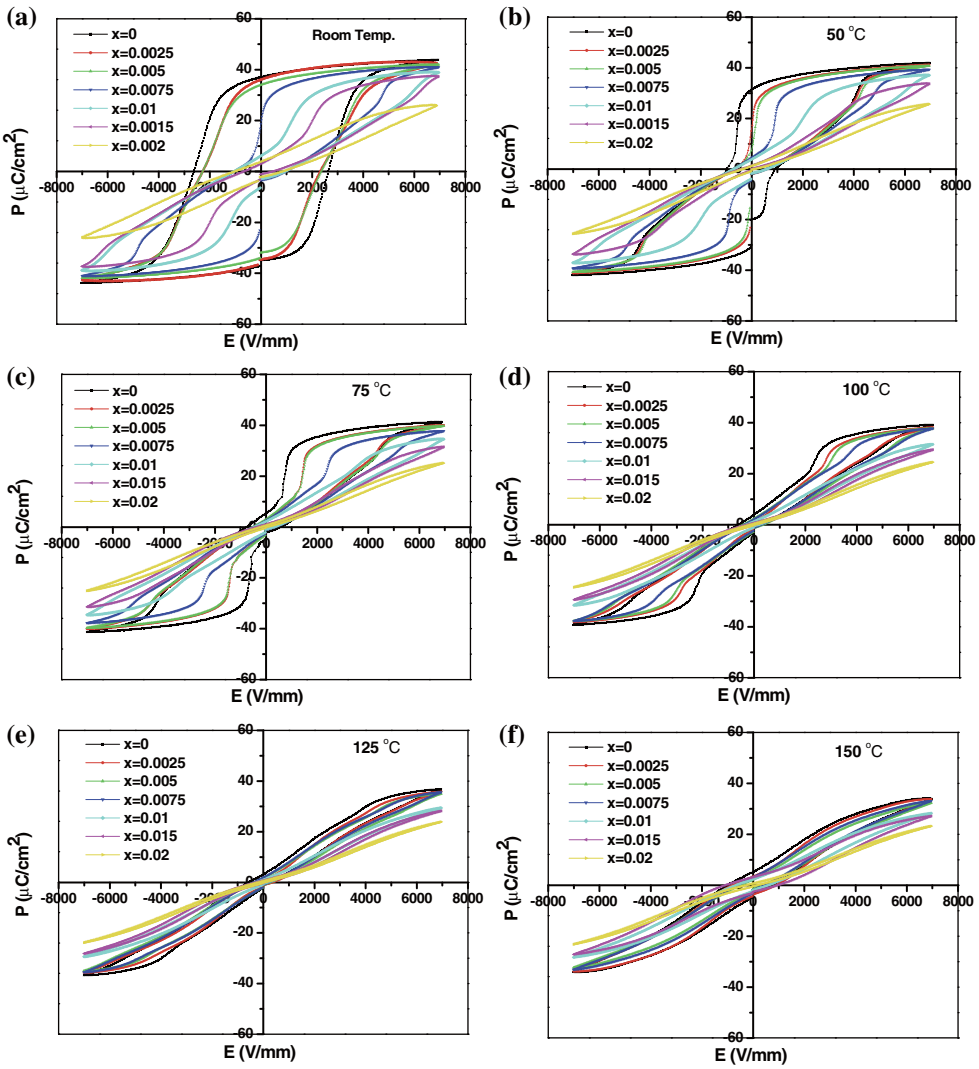

Fig. 6 *P–E* hysteresis loops of BNTBT6 + *x*Nb ceramics measured at various temperatures

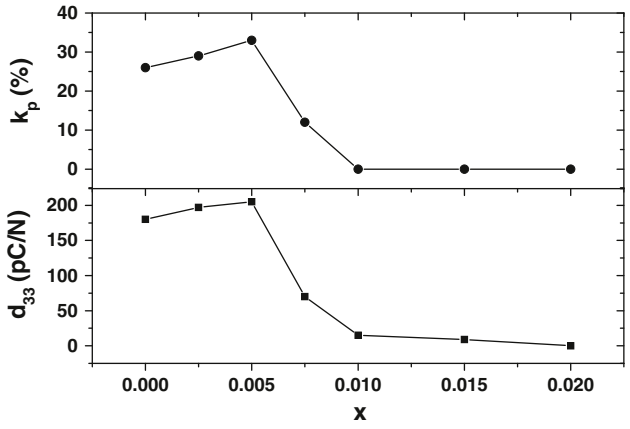

Fig. 7 Piezoelectric properties of BNTBT6 + *x*Nb ceramics as a function of Nb^{5+} content *x*

previously reported for BNTBT compositions. It can be further demonstrated that the citrate sol–gel method is an advantageous alternative to the conventional solid-state method. The reasons could be associated with not only high chemical homogeneity but also dense and fine microstructures. In addition, the substitution of Nb^{5+} for Ti^{4+} might produce A-site vacancies, facilitating the movement of the domain wall and contributing to the piezoelectric properties as well.

Conclusions

The BNTBT6 + *x*Nb ceramics have been successfully prepared by an improved citrate sol–gel method. The sintering behavior, microstructure, and electrical properties of BNTBT6 + *x*Nb lead-free ceramics were studied in detail. It was found that the addition of Nb^{5+} not only influences the densification, but also leads to remarkable changes in dielectric, ferroelectric, and piezoelectric properties. The transition from ferroelectric to anti-ferroelectric phase of BNTBT6 + *x*Nb ceramics is strongly dependent on the

Nb^{5+} content and temperature. Enhanced piezoelectric and electromechanical coupling properties can be achieved in BNTBT6 + *x*Nb ceramics based on a donor doping effect, improved chemical homogeneity, and densification behavior.

Acknowledgements This study was financially supported by Key Project of the Natural Science Research of Universities in Anhui Province (KJ2009A089), a project of the Natural Science Foundation of Anhui Province (090414179), by the National Natural Science Foundation of China (50972035), and a Program for New Century Excellent Talents in University, State Education Ministry (NCET-08-0766).

References

1. Takenaka T, Maruyama K, Sakata K (1991) Jpn J Appl Phys 30:2236
2. Li HD, Feng CD, Yao WL (2004) Mater Lett 58:1194
3. Wang XX, Chan HLW, Choy CL (2005) Appl Phys A 80:333
4. Li HD, Feng CD, Xiang PH (2003) Jpn J Appl Phys 42:7387
5. Zhou XY, Gu HS, Wang Y, Li WY, Zhou TS (2005) Mater Lett 59:1649
6. Chen M, Xu Q, Kim BH, Ahu BK, Chen W (2008) Mater Res Bull 43:1420
7. Zuo RZ, Ye C, Fang XS, Li JW (2008) J Eur Ceram Soc 28:871
8. Chu BJ, Chen DR, Li GR, Yin QR (2002) J Eur Ceram Soc 22:2115
9. Zhao ML, Wang CL, Wang JF, Chen HC, Zhong LW (2004) Acta Phys Sin 53:2357
10. Jing X, Li Y, Yin Q (2003) Mater Sci Eng B 99:506
11. van Hal HAM, Groen WA, Maassen S, Keur WC (2001) J Eur Ceram Soc 21:1689
12. Hou JG, Qu YF, Ma WB, Shan D (2007) J Mater Sci 42:6787. doi:10.1007/s10853-006-1429-1
13. Villegas M, Moure C, Jurano JR, Duran P (1994) J Mater Sci 29:4975. doi:10.1007/BF01151087
14. Yoon SJ, Joshi A, Uchino K (1997) J Am Ceram Soc 80:1035
15. Pookmanee P, Rujijanagul G, Ananta S, Heimann Robert B, Phanichphant S (2004) J Eur Ceram Soc 24:517
16. Mercadelli E, Galassi C, Costa AL, Albonetti S, Sanson A (2008) J Sol–Gel Sci Technol 46:39
17. Shannon RD (1976) Acta Cryst A32:751